High energy shock waves and 5-aminolevulinic for sonodynamic therapy: effects in a syngeneic model of colon cancer

Original Article

High energy shock waves and 5-aminolevulinic for sonodynamic therapy: effects in a syngeneic model of colon cancer

Loredana Serpe, M.D., Ph.D. [1] Roberto Canaparo, Ph.D.[1] Laura Berta, M.D.[2] Alessandro Bargoni, M.D. [2] Gian Paolo Zara, M.D.[1] Roberto Frairia, M.D.[2*]

[1]Department of Anatomy, Pharmacology and Forensic Medicine, University of Torino, Via P. Giuria 13, 10125 Torino, Italy

[2]Department of Clinical Pathophysiology, University of Torino, Via Genova 3, 10126 Torino, Italy

***Corresponding author**

Roberto Frairia, M.D.

Department of Clinical Pathophysiology, University of Torino

Via Genova 3, 10126 Torino, Italy

Tel.: +390116705391 Fax: +390116705366 e-mail: roberto.frairia@unito.it

Short running title

HESW for sonodynamic therapy.

Key words

Sonodynamic therapy; High energy shock waves ; 5-aminolevulinic acid; Colon cancer.

Abbreviations

HESW, High energy shock waves; ALA, 5-aminolevulinic acid; PPIX, protoporphyrin IX; PDT, photodynamic therapy; EFD, energy flux density; TUNEL, terminal deoxynucleotidyltransferase-mediated dUTP nick end labelling; PARP, poly(ADP-ribose)-polymerase.

Abstract

The cytotoxic effect of the natural porphyrin precursor 5-aminolevulinic acid (ALA) exposed to high energy shock waves (HESW) was investigated *in vitro* on DHD/K12/TRb rat colon cancer cells and *in vivo* on a syngeneic colon cancer model.

In vitro, viable cell growth was determined by trypan blue exclusion assay and cell death was investigated by flow cytometry. ALA (50 μg/ml) and HESW (E1, EFD = 0.22 mJ/mm^2, 1000 shots or E2, EFD = 0.88 mJ/mm^2, 500 shots) showed a significant reduction of cancer cell proliferation at day 3 compared to cells exposed to ALA ($p<0.01$) or HESW ($p<0.001$) alone. An enhancement of necrotic and apoptotic cells was observed after combined treatment at day 1 with ALA and HESW E1 (a 3.1 and 6.4 fold increase *vs* ALA alone) or E2 (a 3.4 and 5.3 fold increase *vs* ALA alone).

In vivo, apoptosis detection was carried out by TUNEL assay, the pro-apoptotic gene *Bad* and *Bcl-2* mRNA expression was evaluated by quantitative SYBR Green real time RT-PCR and cleavage of poly(ADP-ribose)-polymerase (PARP) was investigated by Western Blotting. An enhancement of apoptosis was observed in tumour tissues after the combined treatment at day 1 with ALA (375 mg/kg i.v.) and HESW (E2) compared to that of ALA exposure alone with improved apoptotic index (a 2.0 fold increase), *Bad* enhanced mRNA expression ($p<0.01$), *Bcl-2* decreased mRNA expression ($p<0.05$) and increased PARP cleavage. The interaction between HESW and ALA is then effective in inducing apoptosis on a syngeneic colon cancer model.

Introduction

The natural porphyrin precursor 5-aminolevulinic acid (ALA) enters the endogenous heme synthesis pathway, the final step of which occurs in the mitochondria and involves the incorporation of Fe^{2+} into protoporphyrin IX (PPIX) to produce heme (1). In normal cells, PPIX, a substance with excellent photosensitizing properties, does not accumulate to a great extent because it is quickly transformed to heme by the ferrochelatase action of Heme, which is photodynamically inactive. It then undergoes rapid degeneration by heme oxygenase. However, in cancer cells, PPIX accumulates due to a defective heme biosynthesis, hypothesised to be a result of abnormal levels of some of the enzymes involved in this pathway, especially since increased activity of porphobilinogen deaminase and/or decreased activity of ferrochelatase has been reported for a number of tumours (2,3). The exogenous application of ALA may then lead to a pronounced accumulation of PPIX in tumour tissue and subsequent irradiation with light of wavelengths corresponding to the PPIX absorption bands can lead to specific destruction of tumour cells (4).

Although the last 25 years have witnessed the advent of photodynamic therapy (PDT) as an innovative clinical cancer treatment modality the shallow penetration of light through the skin and tissues limits PDT to the treatment of superficial endoscopically reachable tumours (5). Sonodynamic therapy is an analogous approach, based on the synergistic effect of ultrasound and chemical compounds, known as “sonosensitizer”. However, the attractive feature of this modality for cancer treatment emerges from the ability to focus the ultrasound energy on malignancy sites lying deeply within tissues (6). It has already been reported that high energy shock waves (HESW) generated by a piezoelectric device induce acoustic cavitation, which results in a concentration of energy that suffices to generate a sonoluminescence emission, able to elicit electronic excitation of porphyrins by energy transfer and initiate a photochemical process leading to the formation of the cytotoxic singlet oxygen (6,7).

Several studies have been conducted *in vitro* and *in vivo* to investigate the cytotoxic effect of the combination of hematoporphyrin, the most common photodynamic sensitizer and ultrasounds, with encouraging results (8-12). Although ALA and HESW has been reported to be effective *in vitro* against a wide range of cancer cell lines (6,13,14), few studies have been conducted in *in vivo* models (6,10). Therefore, this study has attempted to elucidate the possible efficacy of ALA and HESW treatment *in vivo* and for this purpose, various aspects related to apoptosis have been examined in a BD-IX rat colon cancer model.

Materials and Methods

Cell culture

The rat colon carcinoma cell line, DHD/K12/TRb (PROb), was obtained from the European Collection of Cell Cultures (ECACC, Salisbury, UK). The DHD/K12 cell line is an established transplantable carcinoma cell line, originating from a 1,2-dimethylhydralazine-induced colon adenocarcinoma in BD-IX rats (15). The subline PROb causes progressive tumours in syngeneic rats when inoculated (16). Cells were maintained in culture in Dulbecco's modified Eagle's medium (DMEM, Sigma, St Louis, MO, USA) supplemented with 10% heat-inactivated fetal calf serum (FCS), 2 mM L-glutamine, 100 UI/ml penicillin, 100 µg/ml streptomycin (Sigma) and at 37 °C in a humidified atmosphere of 5% CO_2-air.

In vitro shock wave exposure

A piezoelectric shock wave generator (Piezoson 100, Richard Wolf, Knittlingen, Germany), provided by Med & Sport 2000 S.r.l., Torino, Italy was used for the study. This device generates focused underwater shock waves at various frequencies (1–4 shocks/s) and intensities (0.05–1.48 mJ/mm^2). The energy at the focal point is defined as energy flux density (EFD) per impulse, recorded as joules per area (mJ/mm^2) (17). The axial and lateral dimensions are used to calculate the volume of the focus, simplified under the assumption of an elliptical focus ‘cigar’ where the long axis lies in the direction of the shock wave propagation. The focus volume is defined as the zone where 50% of the maximum energy is delivered (18). As to the Piezoson 100, the focus zone has a length of 10 mm in the direction of the axis of the shock wave propagation and a diameter of 2.5 mm perpendicular to this axis.

Aliquots of 1 ml of cell suspension adjusted to 1×10^6 cell/ml were placed into 2 ml polypropylene tubes (Corning, New York, USA), which were then completely filled with culture medium, for the

in vitro experiments. Subsequently, cells were gently pelleted by centrifugation at 250*g*, so as to minimize motion during shock wave treatment. The experimental set-up was carried out as previously described (19). Two HESW treatment schedules were then investigated: E1, characterized by an EFD of 0.22 mJ/mm^2 and a peak positive pressure of 31 MPa (1000 shots; frequency: 4 shocks/s) and E2, characterized by an EFD of 0.88 mJ/mm^2 and a peak positive pressure of 90 MPa (500 shots; frequency: 4 shocks/s).

In vitro 5-aminolevulinic acid exposure

DHD/K12/TRb cells in the exponential growth phase were preincubated in DMEM, supplemented with 1% FCS containing ALA (10-100 μg/ml) (Sigma, St Louis, MO, USA) for 24 h, then removed from the flask with 0.05% trypsin-0.02% EDTA solution and normalized to 1x10^6 cells. The intracellular fluorescence, determined by the photodynamical active substance PPIX, after cell exposure to the precursor ALA, was evaluated by flow cytometer so as to establish the most suitable concentration for the study (i.e. the concentration reaching over 50% of cell population without significantly affecting cell viability). Control and ALA-treated (50 μg/ml) cells were then exposed to HESW treatment, as described above.

In vitro protocol

To determine cell viability, control cells (i.e. cells receiving no ALA or HESW treatment), cells treated with ALA (i.e. preincubated with ALA 50 μg/ml for 24 h), cells treated with HESW (E1, EFD = 0.22 mJ/mm^2, 1000 shots; and E2, EFD = 0.88 mJ/mm^2, 500 shots) and their combination, were normalized at 25,000 cells/ml, seeded in 24 well/plate in DMEM medium with 10% FCS and subcultured in standard culture conditions for 7 consecutive days. At days 1, 3 and 7, cells were detached with trypsin/EDTA and viable cell growth was determined by trypan blue die exclusion. Viability was expressed as percentage of control cells. Cell viability assay was performed in triplicate.

To analyses cell death, DHD/K12/TRb cells were handled and treated according to the protocol laid out in the Annexin-V-Fluorescin (A-V-FITC) Apoptosis Detection Kit (Sigma). The cells ($1x10^6$ cells/ml), whether preincubated or not with ALA 50 μg/ml for 24 h, were exposed to HESW (E1, EFD = 0.22 mJ/mm^2, 1000 shots and E2, EFD = 0.88 mJ/mm^2, 500 shots) and washed once with PBS to be re-suspended in a binding buffer. A 500 μl aliquot of cell suspension was protected from light and stained with 5 μl of A-V-FITC and 10 μl of propidium iodide (PI) in a 12x75 mm test tube (Corning, New York, USA) for 10 min at room temperature. The cells were then analysed using an EPICS XL flow cytometer (Coulter Corp., Hialeah, FL, USA) by counting 10,000 events. Viable cells were defined as A-V-FITC and PI negative. Cell death analysis was performed in triplicate.

In vivo shock wave exposure

The same piezoelectric shock wave generator used for *in vitro* experiments was employed for the *in vivo* experiments. Tumour bearing rats were anesthetized with an intraperitoneal injection of zolazepam (50 mg/kg) (Zoletil®, Virbac Laboratories) on week 8 after DHD/K12/TRb inoculation. The animals treated with HESW E2 (0.88 mJ/mm^2, 500 shots) were fixed to a board in a supine position, the abdomen shaved and ultrasound gel applied to the naked skin. The transducer was then placed in close contact with the tumour. Following sonographic prelocation, the position and angle of the transducer were adjusted to locate the tumour at the focal spot, thus allowing for focused shock waves to propagate throughout the cancer. All animals were placed on a warm blanket and observed until their complete recovery, before being put back into their cages.

Animals treated with ALA, or on the combination treatment, were given an i.v. injection of ALA before being exposed to the HESW. All animals were sacrificed 24 h after the HESW *in vivo* session and primary tumours were removed, weighed and stored in 10% buffered formalin for

histological examination, in RNAlater (Sigma) for RNA isolation and in TRI Reagent (Sigma) for protein isolation.

In vivo protocol

Syngeneic adult BD-IX male rats, weighing 200 to 250 g, were obtained from Charles River Italia (Milano, Italy). The animals were housed in temperature- and humidity-controlled rooms with a 12 h light/dark cycle and allowed free access to food and water. They were handled according to European guidelines (Directive CEE 86/609) and the experimental protocol was reviewed and approved by the Animal Ethic Committee of the University of Torino, Italy.

Before inoculation, DHD/K12/TRb cells, grown in serum-containing medium, were washed with Hank's balanced buffer and centrifuged at 1500 rpm for 5 min. Cell pellets ($1x10^6$ cells) were re-suspended in 0.15 ml of phosphate-buffered saline (PBS). Each animal was weighed and anaesthetized with an intraperitoneal injection of zolazepam (50 mg/kg) (Zoletil®, Virbac Laboratories, Carros, France). A laparotomy of 2 cm on average was then performed and the caecum isolated. An intramural injection of $1x10^6$ cells in 0.15 ml of PBS was given in the caecum 0.5 cm through the iliocaecal valve.

Eight weeks after cancer cell implantation, the animals were randomly assigned to four treatment groups, with at least four animals per group. Control and experimental animals were treated with one single saline i.v. injection into the tail vein, a single ALA i.v. injection into the tail vein (375 mg/kg), HESW E2 (0.88 mJ/mm^2, 500 shots) or a combination of ALA and HESW E2 (375 mg/kg + 0.88 mJ/mm^2, 500 shots). ALA was dissolved in PBS at a concentration of 80 mg/ml. This solution was injected into a tail vein 3 h before HESW treatment, resulting in a ALA dose of 375 mg/kg (total injection volume per rat approximately 1 ml). An equivalent volume of PBS was

administered to the control animals. The ALA dose used was selected on the basis of the one which showed the greatest inhibitory effect on tumour growth concurrent with low general toxicity (4).

All control and experimental animals were sacrificed 24 h post HESW treatment, examined and scored for the development of macroscopic tumour metastases in various tissues. Primary tumour tissues were then removed for histological examination. The tumour masses of both control and experimental animals were measured in two dimensions by callipers and the tumour volume (V) was calculated by the formula $V=4/3\pi r^3$, r being the mean of the two orthogonal radii.

Haematoxylin-eosin staining and TUNEL analysis

After extensive washing, the fixed tissue fragments were dehydrated through a graded series of ethanol solutions and then passed in xylene and embedded in paraffin before making histological sections. Specimens (4 μm) were washed in xylene and dehydrated according to standard protocols. Sections were either stained with haematoxylin-eosin, or used for terminal deoxynucleotidyltransferase-mediated dUTP nick end labelling (TUNEL), which was carried out using the In Situ Cell Death Detection Kit, POD, (Roche, Indianapolis, USA) according to the manufacturer's instructions.

Briefly, the sections were deparaffinized and the samples pre-treated with 20 μg/ml proteinase K (Roche) for 25 min at 37°C and incubated with TUNEL reaction mixture (terminal deoxynucleotidyl transferase, FITC-labelled nucleotides) for 1 h and covered with peroxidase conjugated anti-fluorescein antibody for 30 min at 37°C. The substrate colour reaction applying chromogen DAB (3,3'-diaminobenzidine tetrahydrochloride) (Roche) was added to the samples for 10 min. Endogenous peroxidase activity was blocked by incubation with 1.3% H_2O_2 in PBS for 10 min at room temperature, before enzymatic labelling. All slides were counter-stained using Meyer haematoxylin.

The classical morphological apoptosis criteria of nuclear condensation, membrane blebbing and the formation of apoptotic bodies, combined with TUNEL-positive reaction of the nuclei, were used to evaluate apoptosis by light microscopy. The apoptotic index was expressed as a percentage of TUNEL-positive cells per total counted cells in random fields, with a minimum of five fields counted per slide, at 40x magnification.

RNA isolation and SYBR Green real time RT-PCR

The RNA was isolated by homogenising tumour samples which were then directly subjected to total RNA isolation by TRI Reagent (Sigma), according to the manufacture's instructions. The RNA concentrations were measured at spectophotometry at 260 and 280 nm with correction for background, at 300 nm. The integrity of the RNA was confirmed by assessing the clarity of the ribosomal bands on ethidium-stained agarose. QuantiTect Primer Assay (Qiagen, Milano, Italy) was used as the gene-specific primer pair for *BAD* (Cat. No. QT00190407) and *BCL-2* (Cat. No. QT00184863). Quantitative RT-PCR was performed using the QuantiTect SYBR Green RT-PCR Kit (Qiagen). Real-time RT-PCR analysis was carried out using 1 μg of total RNA, which was reverse transcribed in a 20 μl complementary deoxyribonucleic acid (cDNA) reaction using the QuantiTect Reverse Transcription Kit (Qiagen), 100 ng of cDNA was used for each 25 μl real-time RT-PCR reaction.

The housekeeping *GAPDH* (Cat. No. QT00199633) gene transcript and real-time PCR was performed by an iQ5 real-time PCR detection system (BIO-RAD, Milano, Italy) to normalise mRNA data. The PCR protocol conditions were as follows: HotStarTaq DNA polymerase activation step at 95°C for 15 min, followed by 40 cycles at various temperatures/times: i.e. 94°C for 15 sec, 55°C for 30 sec and 72°C for 30 sec. All samples were run in duplicate. At least two non-template controls were included in all PCR runs. At the end of the PCR, baseline and threshold

values (C_T) for *BAD, BCL-2* and *GAPDH* were set using the iQ5 real-time PCR Software and the calculated C_T values were exported to Microsoft Excel for analysis. The relative expression of *BAD* and *BCL-2* mRNA was calculated using the comparative C_T method, according to the manufacturer's literature (BIO-RAD).

The relative amount of *BAD* and *BCL-2* mRNA, standardised against the amount of *GAPDH* mRNA, in tissues was expressed as $-\Delta C_T=[C_{T\ BAD/BCL\text{-}2}-C_{T\ GAPDH}]$. The ratio of *BAD* or *BCL-2* mRNA/*GAPDH* mRNA, i.e. the relative *BAD* or *BCL-2* expression, was then calculated as $2^{-\Delta C_T}$. The independent *t* test was used to analyse the differences of *BAD* and *BCL-2* mRNA expression in the various groups.

PARP cleavage assay

Proteins were isolated by homogenising tumour samples, which were then directly subjected to total protein isolation by TRI Reagent (Sigma), according to the manufacture's instructions. The protein concentrations were measured by the Bradford assay. Poly(ADP-ribose)-polymerase (PARP) cleavage were analyzed by immunoblotting. Proteins were subjected to SDS-PAGE (NuPAGE, Invitrogen) and electroblotted to a nitrocellulose membrane (Sigma). Membrane was probed with the following primary antibody: rabbit polyclonal antibody anti-poly-(ADP-ribose)-polymerase (Sigma). Intact and cleaved PARP (116 and 89 kDa, respectively) were detected using ProteoQwest Colorimetric Western Blotting Kit with TMB substrate (Sigma) according to the manufacturer's recommendations.

Data analyses

Data are expressed throughout as mean ± SD. Statistical comparisons between treatment groups were performed with analysis of variance (one-way ANOVA) and the threshold of significance was calculated by Bonferroni's test. Statistical significance was set at $p<0.05$.

Results

In vitro effect on DHD/K12/TRb cells

As shown in Table I, ALA exposure for 24 h had no effect on DHD/K12/TRb cell viability up to 50 μg/ml. Moreover, a significant increase in mean cell fluorenscence intensity (MFI) ($p<0.001$) was observed after exposure to ALA at 50 μg/ml and more than 50% of the cell population were able to synthesize and accumulate the fluorescent photosensitizer PPIX.

The effect on cell viability after HESW exposure was then evaluated at days 1, 3 and 7, after cell exposure to ALA at 50 μg/ml for 24 h. HESW either E1 (EFD = 0.22 mJ/mm^2, 1000 shots) or E2 (EFD = 0.88 mJ/mm^2, 500 shots) treatment alone had no effect on DHD/K12/TRb cell viability at days 1, 3 or 7. At day 1, ALA treatment alone had no effect on cell viability, while the combined treatment (ALA and HESW) led to a significant reduction of DHD/K12/TRb cell viability ($p<0.01$). At day 3, ALA treatment alone effected cell viability ($p<0.01$) and the combined treatment led to a marked reduction in cell viability ($p<0.001$) (Figure 1). At day 7, a decreased reduction in DHD/K12/TRb cell viability after either ALA treatment alone or combined treatment was observed ($p<0.05$ and $p<0.01$, respectively).

So as to further explore the increasing cytotoxic effect of HESW treatment on ALA treated cells, DHD/K12/TRb cell death was evaluated by annexin V/propidium iodide assay at day 1. The HESW (E1 and E2), or ALA treatment alone led to a similar percentage of necrotic and apoptotic cells as did untreated cells, indicating that ALA or HESW treatment alone did not induce either cell necrosis or apoptosis. Conversely there was a significant increase in both necrotic and apoptotic cells after the combined ALA and HESW E1 treatment (36.8 and 42.8%, respectively) or E2 (40.2 and 35.4%, respectively), compared to the necrotic and apoptotic cell percentage obtained by treatment with ALA alone (11.0 and 6.7%, respectively) and HESW E1 (8.4 and 4.6%,

respectively) or E2 alone (10.5 and 6.0%, respectively) (Figure 2). Therefore, HESW treatment determined a significant enhancement of ALA induced necrosis and apoptosis in DHD/K12/TRb cells.

In vivo effect on DHD/K12/TRb tumours

Eight weeks after DHD/K12/TRb cell inoculation, animals in the control group were treated with one single saline i.v. injection into the tail vein, whereas the experimental animal group was treated with a single ALA i.v. injection into the tail vein (375 mg/kg, 3 h before shock wave exposure), HESW E2 (0.88 mJ/mm^2, 500 shots) or an ALA and HESW combination treatment. The cytotoxic effect of the treatments was evaluated by measuring the percentage of apoptotic cells in the DHD/K12/TRb tumours with nuclear fragment DNA staining, using the TUNEL method and histological examination of haematoxylin-eosin stained sections at 24 h post-HESW treatment.

The tumour volume averaged 2923±97 mm^3 and the mean tumour volume did not differ significantly from that of the control animals.

The TUNEL analysis showed that the combined ALA HESW treatment induced a significant increase in the apoptotic index (6.9 ± 1.1%) versus the control group (1.8 ±0.2%; $p<0.01$), the HESW group (3.7 ± 0.5%; $p<0.01$) and versus the ALA group (3.9 ± 0.7%; $p<0.05$) (Figure 3). Conversely, neither ALA nor HESW treatment alone produced a significant change in the apoptotic index of cancerous cells versus the control group. As already observed in *in vitro* experiments, HESW treatment may trigger ALA cytotoxicity in colon cancer tumour. Histological examination of the haematoxylin-eosin sections from ALA + HESW treated animals showed larger areas of tumour necrosis, confirming the TUNEL analysis findings (Figure 4).

In vivo effect on apoptotic gene expression

Real time RT-PCR analysis was used to confirm the apoptotic pathways expressed by the TUNEL analysis, investigating the mRNA expression of the pro-apoptotic *BAD* and anti-apoptotic *BCL-2* gene involved in the apoptotic machinery. Figure 5 shows that mRNA expression of *BAD* was enhanced whilst the mRNA expression of *BCL-2* was lower in the animals treated with ALA and HESW compared to the control animals ($p<0.05$). When a comparison was made with the control group, it was observed that, in the ALA and HESW treated group, the *BAD* mRNA steady-state level was up-regulated, with 2.4 fold increase, whilst the *BCL-2* mRNA steady-state level was down-regulated with 4.5 fold decrease. As shown in Figure 5, in the ALA and HESW group versus the ALA group, the *BAD* mRNA steady-state level was also up-regulated, with a 2.0 fold increase, whilst the BCL-2 mRNA steady-state level was down-regulated with a 2.0 fold decrease.

In vivo effect on PARP cleavage

Western Blotting was used to check whether DHD/K12/TRb tumours in BD-IX rats exposed to ALA (375 mg/kg, i.v.) or/and HESW E2 (0.88 mJ/mm^2, 500 shots) treatment express any hallmarks of the apoptotic process i.e. specific cleavage of PARP into 89 kDa fragment, as marker of activation of caspases. At 24 h post-treatment, PARP cleavage was evident after ALA treatment alone in only one of the four tumour tissues exposed, likewise after HESW E2 treatment alone and in three of the four tumour tissues exposed after the combined treatment with ALA and HESW E2 (Figure 6).

Discussion

Sonodynamic therapy has been suggested as an innovative modality for cancer treatment, as it is able to enhance the cytotoxic activities of compounds defined as sonosensitizers. The main assumption about the sonodynamic therapy is to generate ultrasound energy which produces sonoluminescence to excite the hematoporphyrin derivative by energy transfer. This initiates a photochemical process which leads to the formation of the cytotoxic singlet oxygen (20).

Shock waves can propagate through different substances without significant energy dissipation as long as the acoustic impedance values of the substances are similar. Because of the similarity in the acoustic impedance values of water and the soft tissues of the body, shock waves can be transmitted through these tissues without any substantial energy loss. However, at transition sites between tissues with different acoustic impedance values, energy dissipation occurs and there may be focal mechanical destruction, probably produced through the induction of cavitation and shearing stress caused by the reflected waves (21).

In a previous study we investigated in a human colon cancer cell line, HT-29, which was exposed to ALA, the effects a piezoelectric device able to generate pulse HESW with two basic effects: the direct generation of mechanical forces (non-inertial cavitation) and the indirect generation of mechanical forces by cavitation (inertial cavitation). Non-inertial cavitation bubbles oscillate about an equilibrium radius and often persist through many acoustic cycles. These oscillations cause streaming of the surrounding liquid and mechanical stresses to create a mixing of the medium. Inertial cavitation is an extremely violent process of bubble activity that may lead to pyrolysis of the water vapour inside the bubble, generating highly reactive hydroxyl radical and hydrogen atoms. Inertial cavitation can also be followed by energy transfer to oxygen to generate the highly reactive singlet molecular oxygen (6).

This mix between inertial and non-inertial cavitation, generated by our piezoelectric device, was confirmed in our previous study (13), where we demonstrated that combined ALA HESW treatment produced significant inhibition of HT-29 cell growth, where non-inertial cavitation and inertial cavitation were seen to induce apoptosis and inhibit cell growth by increasing the G_0/G_1 population through the intracellular activation of protoporphyrin IX.

So as to further our investigation we evaluated the effect of HESW on DHD/K12/TRb rat colon cancer cells previously exposed to ALA, a natural porphyrin precursor commonly used as sonosensitizer, in a syngeneic model of colon cancer. Our results show that DHD/K12/TRb cells are sensitive to ALA and HESW treatment. The fact that the piezoelectric device used is able to generate different combinations of the two basic effects suggests that HESW E1 and E2 schedules represented a dissimilar mechanism involved in the synergism between ultrasounds and ALA.

ALA exposed to HESW led to a significant reduction of *in vitro* cancer cell proliferation at day 3 compared to cells exposed to ALA ($p<0.01$), or HESW ($p<0.001$) alone. An enhancement of necrotic and apoptotic cells was observed after the combined treatment with ALA and HESW E1 (3.1 and 6.4 fold increase *vs* ALA alone), or E2 (3.4 and 5.3 fold increase *vs* ALA alone). These findings are in agreement with our previous reports, indicating that shock waves have a sudden effect in enhancing cytotoxic activities of compounds defined as sonosensitizers in different cell lines (13,14).

In the BD-IX rat colon cancer model, a significant increase in the apoptotic index of DHD/K12/TRb tumours exposed to the combined treatment compared to controls, HESW and ALA alone was observed by the TUNEL method (Figure 3). Moreover, we investigated the pro-apoptotic gene BAD and anti-apoptotic gene BCL-2 mRNA expression in an effort to better understand the apoptotic pathways triggered. A *Bad* enhanced mRNA expression ($p<0.01$) and *Bcl-2* decreased

mRNA expression ($p<0.05$) was observed in the group exposed to HESW in combination with ALA, compared to that observed with single treatment alone (i.e. ALA or HESW E2) (Figure 5).

PARP is a chromatin-associated enzyme which, in response to DNA damage, binds to DNA strand breaks and undergoes automodification by forming long, branched poly (ADP) ribose polymers (22). In this study, an enhanced PARP cleavage was observed in tumour tissues exposed to the combined treatment compared to those exposed to the single treatment alone (i.e. ALA or HESW), thus confirming that HESW are able to activate ALA.

These data confirm that combined ALA and HESW treatment suppresses cell proliferation and is able to induce apoptosis not only *in vitro,* but also in solid *in vivo* tumours. This finding is also in keeping with results reported by Canaparo *et al* in a syngeneic rat model of breast cancer and by Maruyama *et al* in a mouse hepatoma model (23,24). Several distinct sonochemical effects were observed after sonodynamic treatment with ultrasound in various cell lines, including changes in cell viability, the generation of mitochondrial ROS, mitochondrial swelling and the release of cytochrome c, showing that the ultrasonically-induced cell-killing effect could be enhanced by PPIX (25,26). Moreover, the usefulness of sonodynamic therapy, taking advantage of focused ultrasound and photosensitizer was evidenced in the treatment of experimental sarcoma and malignant glioma (27,28).

In conclusion, HESW might be proposed for the sonodynamic treatment of cancer since the interaction between focused ultrasonic fields and a photosensitizer like ALA is effective in inducing apoptosis in tumours cells. Anyhow, further experiments are needed to support our hypotesis that HESW are able to produce *in vivo* sonoluminescence since we do not have evidence about light emission associated with cavitation mechanism in our syngeneic model of colon cancer.

Acknowledgements

This work was supported by a grant from Compagnia di San Paolo, Torino, Progetto Oncologia (grant number 24366/8651) and by Regione Piemonte, Progetto Ricerca Sanitaria Finalizzata (grant number 10145/27.001/2006).

We thank Prof. Roberto Chiarle and Dr. Ornella Bosco (University of Torino, Italy) for their technical support and Mrs. Barbara Wade for her linguistic advice.

References

1. Ades, I.Z. Heme production in animal tissues: the regulation of biogenesis of delta-aminolevulinate synthase. *Int J Biochem 22*, 565-578 (1999).
2. Gibson, S.L., Cupriks, D.J., Havens, J.J., Nguyen, M.L., Hilf, R. A regulatory role for porphobilinogen deaminase (PBGD) in delta-aminolevulinic acid (delta-ALA)-induced photosensitization? *Br J Cancer 77*, 235-243 (1998).
3. el Sharabasy, M.M., el Waseef, A.M., Hafez, M.M., Salim, S.A. Porphyrin metabolism in some malignant diseases. *Br J Cancer 65*, 409-412 (1992).
4. Frank, J., Lambert, C., Biesalski, H.K., Thews, O., Vaupel, P., Kelleher, D.K. Intensified oxidative and nitrosative stress following combined ALA-based photodynamic therapy and local hypertermia in rat tumors. *Int J Cancer 107* 941-948 (2003).
5. Brown, S.B., Brown, E.A., Walker, I . The present and future role of photodynamic therapy in cancer treatment. *Lancet Oncol 5*, 497-508 (2004).
6. Rosenthal, I., Sostaric, J.Z., Riesz, P. Sonodynamic therapy-a review of the synergistic effects of drugs and ultrasound. *Ultrason Sonochem 11* 349-363 (2004).
7. Tavakkoli, J., Birer, A., Arefiev, A., Prat, F., Chapelon, J.Y., Cathignol, D. A piezocomposite shock wave generator with electronic focusing capability: application for producing cavitation-induced lesions in rabbit liver. *Ultrasound Med Biol 23*, 107-115 (1997).
8. Meunier, A., Guillemin, F., Merlin, J.L., Eikermann, K., Schmitt, S., Stoss, M., Hopfel, D., Barth, G., Bolotina, L. Can ultrasounds induce cytotoxicity in presence of hematoporphyrin derivative as photodynamic therapy? *Proc SPIE Int Soc Opt Eng 2625*, 419 (1996).
9. Umemura, K., Yumita, N., Nishigaki, R., Umemura, S. Sonodynamically induced antitumor effect of a pheophorbide a. *Cancer Letters 102*, 151-157 (1996).

10. Yumita, N., Sasaki, K., Umemura, S., Yukawa, A., Nishigaki, R. Sonodynamically induced antitumor effect of gallium-porphyrin complex by focused ultrasound on experimental kidney tumor. *Cancer Letters 112*, 79-86 (1997).
11. Yumita, N., Nishigaki, R., Umemura, S. Sonodynamically induced antitumor effect of Photofrin II on colon 26 carcinoma. *J Cancer Res Clin Oncol 126*, 601-606 (2000).
12. Yumita, N., Okuyama, N., Sasaki, K., Umemura, S. Sonodynamic therapy on chemically induced mammary tumor: pharmacokinetics, tissue distribution and sonodynamically induced antitumor effect of porfimer sodium. *Cancer Sci 95*, 765-769 (2004).
13. Canaparo, R., Serpe, L., Catalano, M.G., Bosco, O., Zara, G.P., Berta, L., Frairia, R. High energy shock waves (HESW) for sonodynamic therapy: effects on HT-29 human colon cancer cells. *Anticancer Res 26*, 3337-3342 (2006).
14. Catalano, M.G., Costantino, L., Fortunati, N., Bosco, O., Pugliese, M., Boccuzzi, G., Berta, L., Frairia, R. High energy shock waves activate 5-aminolevulinic acid and increase permeability to paclitaxel: antitumor effects of a new combined treatment on anaplastic thyroid cancer cells. *Thyroid 17* 91-99 (2007).
15. Martin, F., Caignard, A., Jeannin, J.F., Leclerc, A., Martin, M. Selection by trypsin of two sublines of rat colon cancer cells forming progressive or regressive tumors. *Int J Cancer 32*, 623 (1983).
16. Martin, M.S., Bastien, H., Martin, F., Michiels, R., Martin, M.R., Justrabo, E. Transplantation of intestinal carcinoma in inbred rats. *Biomedicine 19*, 555 (1973).
17. Folberth, W., Kohler, G., Rohwedder, A., Matura, E. Pressure distribution and energy flow in the focal region of two different electromagnetic shock wave sources. *J Stone Dis 4*, 1–7 (1992).
18. Wess, O., Ueberle, F., Dürßen, R.N., Hileken, D., Krauss, W., Reuner, T., Schultheiss, R., Staudenraus, J., Rattner, M., Haaks, W., Granz, B. Working group technical developments - Consensus report. In: *High Energy Shock Waves in Medicine. Clinical Application in*

Urology, Gastroenterology and Orthopedics, pp. 59–71. Eds., Chaussy, C., Eisenberger, F., Jocham, D., Wilbert, D. Stuttgart; Georg Thieme Verlag (1997).

19. Frairia, R., Catalano, M.G., Fortunati, N., Fazzari, A., Raineri, M., Berta, L. High energy shock waves (HESW) enhance paclitaxel cytotoxicity in MCF-7 cells. *Breast Cancer Res Treat 81*, 11-19 (2003).
20. Noodt, B.B., Berg, K., Stokke, T., Peng, Q., Nesland, J.M. Apoptosis and necrosis induced with light and 5-aminolaevulinic acid-derived protoporphyrin IX. *Br J Cancer 74*, 22-29 (1996).
21. Kato, K., Fujimura, M., Nakagawa, A., Saito, A., Ohki, T., Takayama, K., Tominaga, T. Pressure-dependent effect of shock waves on rat brain: induction of neuronal apoptosis mediated by a caspase-dependent pathway. *J Neurosurg 106*, 667–676 (2007).
22. Lindahl, T., Satoh, M.S., Poirier, G.G., Klungland, A. Posttranslational modification of poly(ADP-ribose) polymerase induced by DNA strand breaks. *Trends Biochem Sci 20*, 405–411 (1995).
23. Canaparo, R., Serpe, L., Zara, G.P., Chiarle, R., Berta, L., Frairia, R. High energy shock waves (HESW) increase paclitaxel efficacy in a syngeneic model of breast cancer. *Technol Cancer Res Treat 7*, 117-124 (2008).
24. Maruyama, M., Asano, T., Nakagohri, T., Uematsu, T., Hasegawa, M., Miyauchi, H., Iwashita, C., Isono, K. Application of high energy shock waves to cancer treatment in combination with cisplatin and ATX-70. *Anticancer Res 19*, 1989-1993 (1999).
25. Hayashi, S., Yamamoto, M., Tachibana, K., Ueno, Y., Bu, G., Fukushima, T. Mechanism of photofrin enhanced ultrasound-induced human glioma cell death. *Anticancer Res 29*, 897-905 (2009).
26. Mi, N., Liu, Q., Wang, X., Zhao, X., Tang, W., Wang, P., Cao, B. Induction of sonodynamic effect with protoporphyrin IX on isolate hepatoma-22 cells. *Ultrasound Med Biol 35* 680-686 (2009).

27. Liu, Q., Wang, X., Wang, P., Xiao, L., Hao, Q. Comparison between sonodynamic effect with protoporphyrin IX and hematoporphyrin on sarcoma 180. *Cancer Chemother Pharmacol 60*, 671-680 (2007).
28. Nonaka, M., Yamamoto, M., Yoshino, S., Umemura, S., Sasaki, K., Fukushima, T. Sonodynamic therapy consisting of focused ultrasound and a photosensitizer causes a selective antitumor effect in a rat intracranial glioma model. *Anticancer Res 29*, 943-950 (2009).

Table I

5-aminolevulinic acid (ALA) effect on mean fluorescence intensity (MFI) and viability of DHD/K12/TRb cells after 24 h exposure

Condition		MFI Ratio	Fluorescent Cells	Viability Ratio
		Ala treated cells/ Control cells	Percentage	Ala treated cells/ Control cells
ALA	25 μg/ml	2.4 **	37.6 ***	1.0
ALA	50 μg/ml	3.6 ***	57.6 ***	1.0
ALA	100 μg/ml	5.8 ***	70.2 ***	0.8 *

Significance versus ALA unexposed cells: * $p<0.05$, ** $p<0.01$; *** $p<0.001$

Figure 1

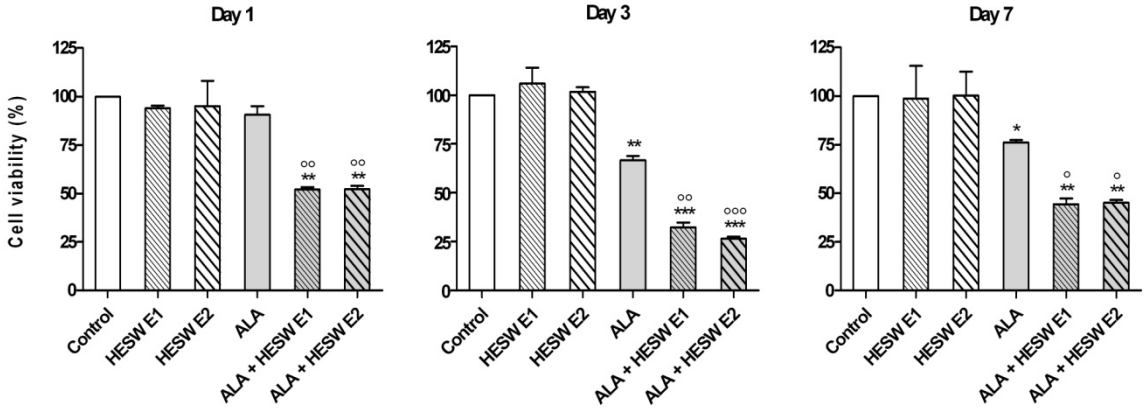
Day 1
Day 3
Day 7
Cell viability (%)
125
100
75
50
25
0
Control
HESW E1
HESW E2
ALA
ALA + HESW E1
ALA + HESW E2
**
°°
***
°°°
*
°

Figure 2

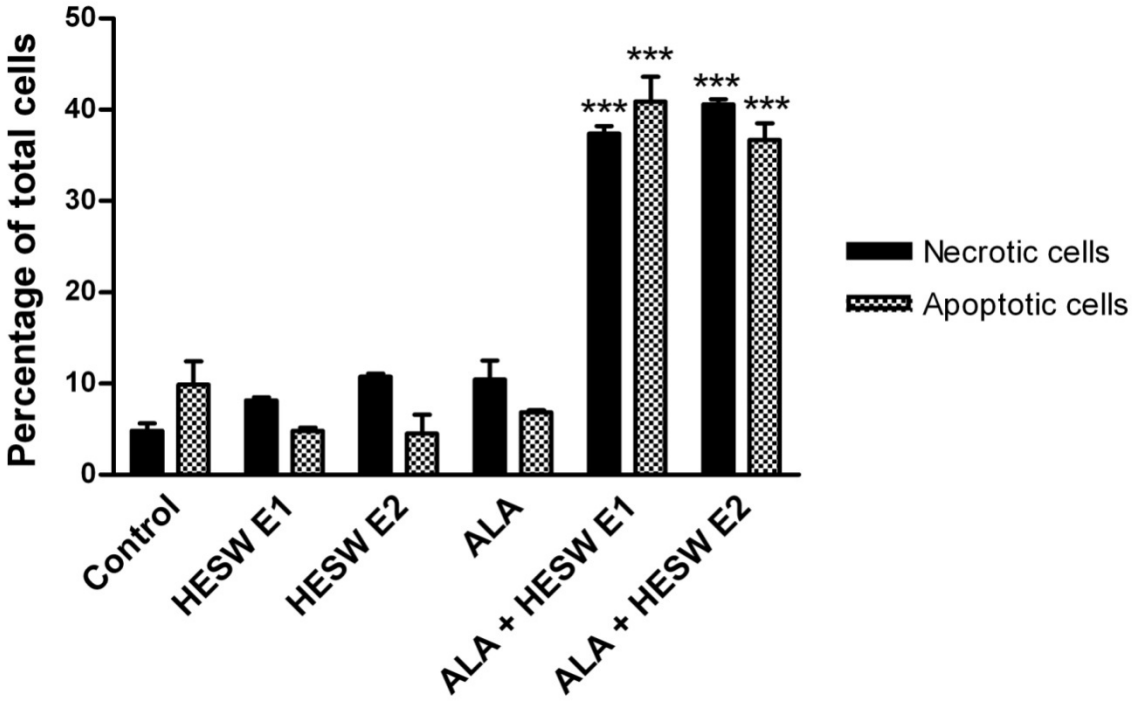
Percentage of total cells
50
40
30
20
10
0
***
***
***
***
Control
HESW E1
HESW E2
ALA
ALA + HESW E1
ALA + HESW E2
Necrotic cells
Apoptotic cells

Figure 3

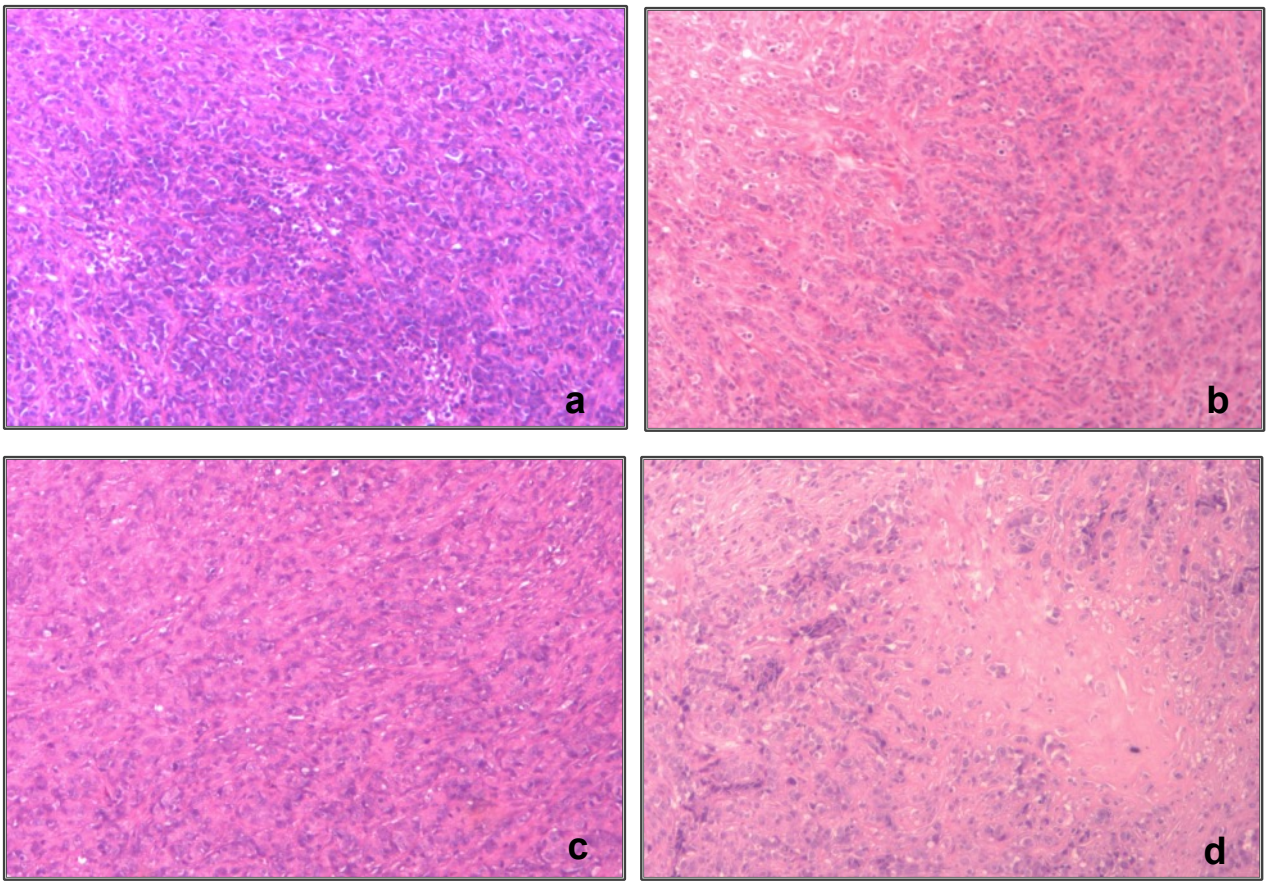

Figure 4

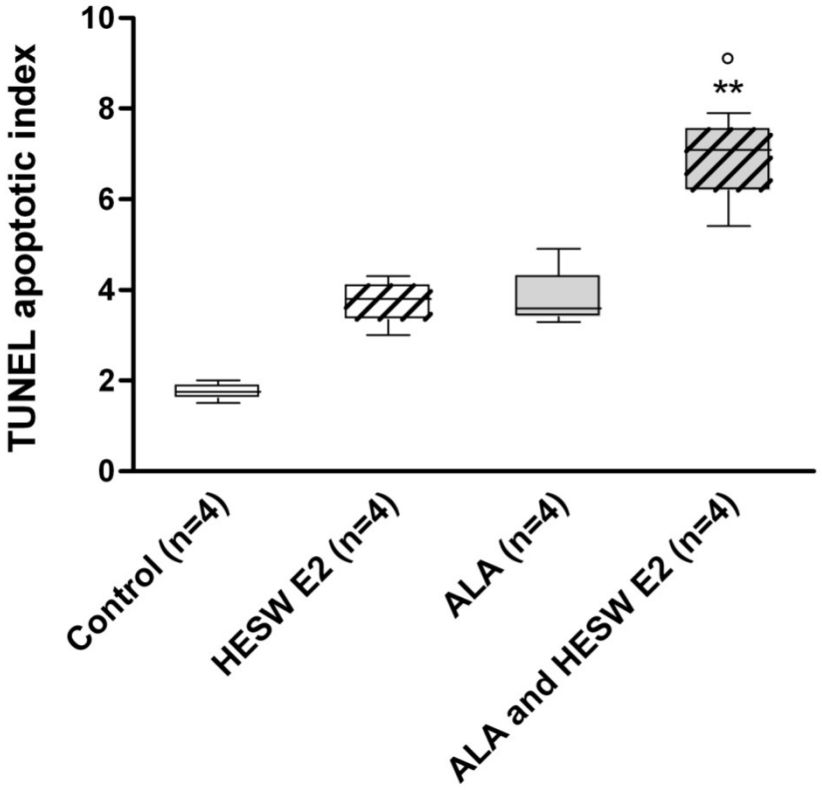
TUNEL apoptotic index
10
8
6
4
2
0
**
Control (n=4)
HESW E2 (n=4)
ALA (n=4)
ALA and HESW E2 (n=4)

Figure 5

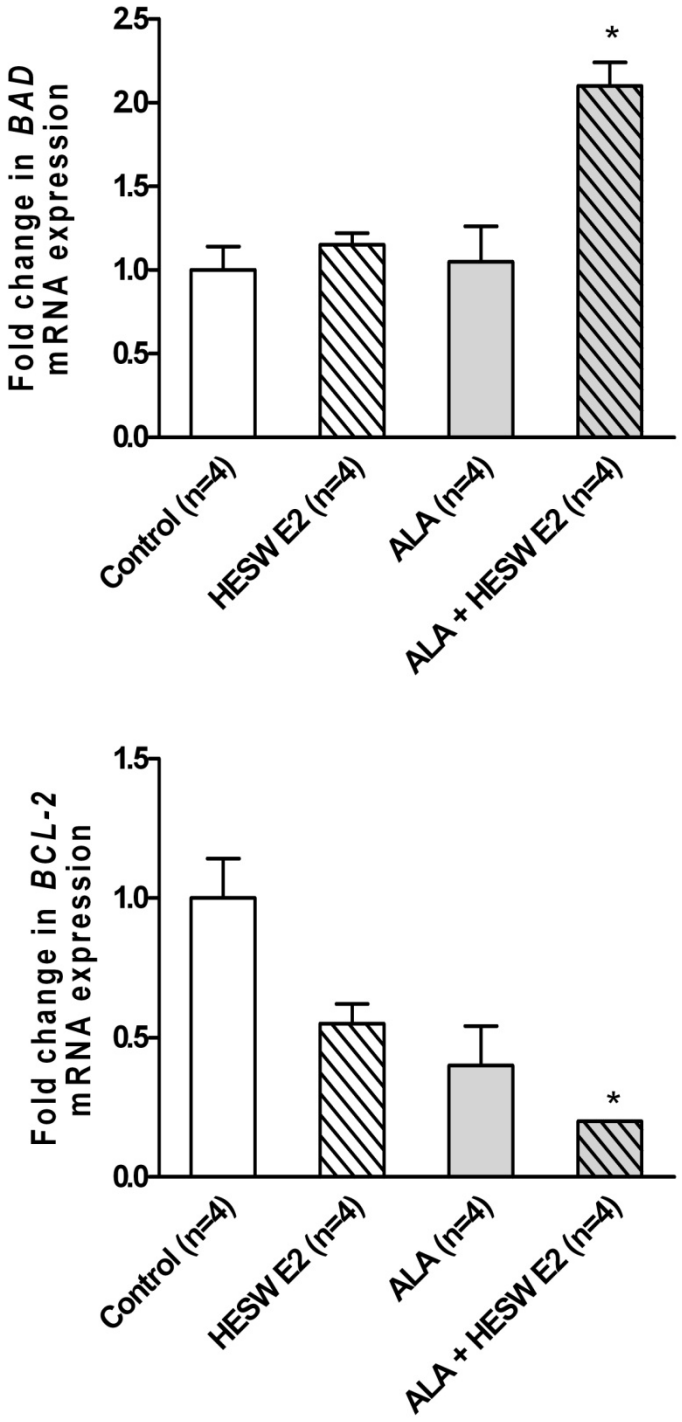
Fold change in BAD mRNA expression
2.5
2.0
1.5
1.0
0.5
0.0
*
Control (n=4)
HESW E2 (n=4)
ALA (n=4)
ALA + HESW E2 (n=4)
Fold change in BCL-2 mRNA expression
1.5
1.0
0.5
0.0
*
Control (n=4)
HESW E2 (n=4)
ALA (n=4)
ALA + HESW E2 (n=4)

Figure 6

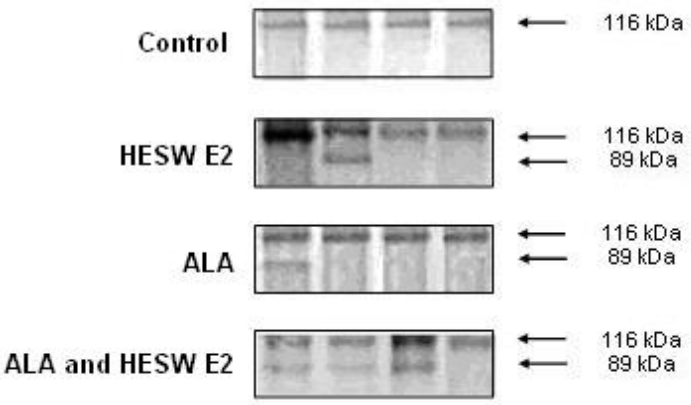
Control
116 kDa
HESW E2
116 kDa
89 kDa
ALA
116 kDa
89 kDa
ALA and HESW E2
116 kDa
89 kDa

Figure Legends

Figure 1

In vitro effect of ALA (50 μg/ml) and HESW (E1, EFD = 0.22 mJ/mm^2, 1000 shots; E2, EFD = 0.88 mJ/mm^2, 500 shots) on DHD/K12/TRb cells at day 1, 3 and 7. Cell viability is determined as the ratio between treated cells and untreated control cells (100%). The results are expressed as mean values ± SD of three independent experiments. Significance versus control cells: * $p<0.05$, ** $p<0.01$, *** $p<0.001$; versus cells exposed to ALA alone: ° $p<0.05$, °° $p<0.01$, °°° $p<0.001$.

Figure 2

In vitro cell necrosis and apoptosis with ALA (50 μg/ml) and HESW (E1, EFD = 0.22 mJ/mm^2, 1000 shots; E2, EFD = 0.88 mJ/mm^2, 500 shots) in DHD/K12/TRb cells at day 1. Data are presented as a percentage of cells in the necrotic or apoptotic state and are mean values ± SD of three independent experiments. Significance versus control cells: *** $p<0.001$.

Figure 3

The morphologic features of the cells in control (a), ALA (375 mg/kg i.v. injection) (b), HESW (E2, 0.88 mJ/mm^2, 500 shots) (c) and combined treatment (ALA + HESW) groups (d). Representative haematoxylin-eosin sections of each group are shown.

The haematoxylin-eosin staining DHD/K12/TRb tumours at 24 h after treatment were examined and photographed under light microscope at a 10x magnification.

Figure 4

In vivo effect of ALA (375 mg/kg i.v. injection) and HESW (E2, 0.88 mJ/mm^2, 500 shots) on DHD/K12/TRb tumours in BD-IX rats at 24 h after combined treatment. Data are presented as apoptotic index determined by the TUNEL analysis as percentage of apoptotic cells per total counted cells in random fields. The results are mean values ± SD. Significance versus control cells: ** $p<0.01$; versus cells exposed to ALA alone: ° $p<0.05$

Figure 5

In vivo effect of ALA (375 mg/kg i.v. injection) and HESW (E2, 0.88 mJ/mm^2, 500 shots) on *BAD* and *BCL-2* mRNA expression in DHD/K12/TRb tumours in BD-IX rats at 24 h after combined treatment by real time RT-PCR. The different transcript level normalized to those of *GAPDH* mRNA expression. Significance versus control cells: * $p<0.05$.

Figure 6

In vivo effect of ALA (375 mg/kg i.v. injection) and HESW (E2, 0.88 mJ/mm^2, 500 shots) on PARP cleavage induction in DHD/K12/TRb tumours in BD-IX rats at 24 h after combined treatment. Protein extracts were subjected to 10% SDS-PAGE and PARP cleavage was assessed by Western Blotting with an anti-PARP antibody (1:1500) which detects intact (116 kDa) and cleaved (89 kDa) products.